ΜΑΘΗΜΑΤΙΚΑ.— **The Equivalent Through-Crack Model for the Surface Part-Through Crack,** *by P. S. Theocaris - D. L. Wu**.

Ἀνεκοινώθη ὑπὸ τοῦ Ἀκαδημαϊκοῦ κ. Περικλῆ Θεοχάρη.

SUMMARY

The three-dimensional problem of a surface part-through cracked plate is reduced to a two-dimensional problem by introducing an equivalent through-crack model, loaded by a convenient tension and bending stress distribution along the lips of the crack. The principle of the model is based on a similar idea as in the *line-spring model*, introduced by Rice and Levy [**1**]. In this model the singularities existing at the extremities of the surface lips of the part-through crack on the near face of the plate, indicated by experiments, were taken into account, whereas, in the line-spring model these extremities were considered as free. According to this model the effect of the surface part-through crack was replaced by a continuous distribution of forces N (x, 0) and moments M (x, 0) along the near-face crack lips applied to an equivalent through crack. These forces and moments were represented by power functions completely determining the boundary conditions along the crack. In this way the two-dimensional problem, derived from the model, can be readily reduced to a well-known Hilbert problem yielding integral equations containing the functions expressing the N (x, 0) — and M (x, 0) — distributions along the length of the crack. These equations were solved by an approximate numerical procedure. From this solution the expressions of stress- and displacement-fields for the surface part-through crack may be evaluated, expressed in terms of the distribution of the stress intensity factor function calculated along the whole front of the equivalent through crack.

INTRODUCTION

Service failures in structures appear at the beginning as surface flaws. This is the reason why this form of cracks, although not being of the most prevalent type, is of great significance as a failure origin. However, the analytic solutions for surface crack-problems of finite-thickness plates have been up-to-now rather poor. Irwin in 1962 [**2**] used a solution of Green and Sneddon [**3**] to evaluate the stress intensity factor for a semi-elliptic surface crack in a half-space. Smith [**4**] developed a solution, based on the

* Π. Σ. ΘΕΟΧΑΡΗ - D. L. WU, **Τὸ ὁμοίωμα τῆς ἰσοδυνάμου διαμπεροῦς ρωγμῆς διὰ τὴν μελέτην τῆς ἐπιφανειακῆς μερικῆς ρωγμῆς.**

so-called alternating method, for a semi-circular surface crack under conditions of K_I-mode deformation and Smith and Alavi [**5**] gave a solution for a circular crack embedded in a half-space, as well as for a circular crack partially contained in the half-space [**6**]. Thresher and Smith [**7**] have refined the work contained in refs. [**5**] and [**6**] and they have determined stress intensity factors in surface part-through cracks of circular contours.

The case of embedded elliptic cracks, which better approximate geometries of actual cracks, was encountered by Shah and Kobayashi [**8**], who evaluated the stress intensity factors there, under arbitrary normal loading of the body, and in ref. [**9**] a study was undertaken to define the influence of approaching the free surface of the semi-infinite solid on the values of the stress intensity factor. Finally, the same authors, in a review paper [**10**], yielded a thorough study of the evaluation of the stress intensity factor in embedded surface or inside part-through elliptic cracks and exposed, in the form of graphs, interesting laws of variation of this quantity.

All these studies were based on an alternating technique, grounded on two particular solutions. The first-one corresponds to the problem of an infinite body containing an internal flat crack (circular or elliptical) and subjected to a variable pressure loading on the crack surface. The second-one corresponds to a semi-infinite body, subjected to convenient normal and shearing fractions on its plane boundary, which counterbalance, by small square rechtangles, the partial resultants of the stresses over each rectangle, introduced by the first solution of the problem.

Hartranft and Sih [**11**] have analyzed the state of stress singularity in the zone of the front face of the plate, where a circular crack penetrates this surface and thus have improved considerably the results of previous investigations.

In some of these solutions, and especially for the cases of elliptic cracks, use was made of a convenient ellipsoidal harmonic function, whose properties were studied by Segedin [**12**], and which represented conveniently any polynomial distribution of pressure on the crack surface. However, mathematical complexities have limited this polynomial distribution of external loading to terms up to the third order. Recently, only Nishioka and Atluri [**28**] and Vijaya Kumar and Atluri [**29**] gave a general solution for an embedded elliptic crack, subject to arbitrary crack-face tractions in an infinite body, and solved the problems of part-through cracks in a finite thickness plate by the alternating method, in conjunction with the finite element method.

On the other hand, three-dimensional finite-element methods were developed [**13**, **31**], but these applications are subject to the already known difficulties of this potential method to define adequately the stress field at the vicinity of the crack tip and the necessity of disposing large memory digital computers. For these reasons they are limited in number.

The *boundary integral equation* method, introduced by Cruse [**15**], was used for the solution of surface part-through cracks [**14**, **16**], but again the method presents some limitations, which make its results at the vicinity of the intersection of the free surface with the crack front doubtful.

The line-spring model method, introduced by Rice and Levy [**1**], yielded an approximate solution of part-through surface cracked plates, which gave more accurate results than any other previous method. On the other hand this method appears to present a versatility for diverse applications in shell structures [**18**] with complicated shapes, where eventually plasticity interferes [**19**].

According to the line-spring model the net ligament stresses along the width of the surface crack are represented by a membrane load (N) and a moment (M) distribution, whereas the crack near-face displacements are expressed in terms of a crack-opening function (δ) and a relative rotation (θ), both referred to the mid-plane of the plate, which are assumed as continuous functions along the length of the crack. The values of these quantities are approximated by the corresponding plane-strain results, corresponding to a series of respective edge-cracked strips of variable depth of the cracks. While the approximation of the stress intensity factor by this model is satisfactory along the central section of the crack, it becomes less appropriate near its ends, where the crack intersects the free surface.

Moreover, at the points where the part-through crack lips intersect the near face of the plate the model assumes a zero value for the respective stress intensity factor, since the length of the corresponding plane-strain edge crack there should be equal to zero.

However, experimental evidence, presented in this paper, indicates clearly that a weak singularity of the stress function exists. Such types of singularities were previously detected and studied in refs. [**20**].

It is the purpose of this paper to introduce an equivalent through-crack model, which may take care of these anomalies of the stress field at the intersection of the crack front with the near face of the plate and yield therefore accurate results for the variation of the stress intensity factor along the whole front of the surface part-through crack.

DEFINITION OF THE EQUIVALENT THROUGH-CRACK MODEL

The configuration of the surface part-through cracked plate, subjected to a uniform tension at infinity, is indicated in Fig. 1. The existence of weak singularities indicated experimentally by the front-face caustics (see Fig. 3a) implied the assumption that the heights of the shallow protrusions at the end points A and B of the front-surface trace of the crack are not zero and they have a dimension of the same order of magnitude of the crack opening displacement at the deformed humps. Then, $\delta(a)$ may be considered as proportional to σ_∞^2, instead of the normally made assumption that $\delta(x)$ at the crack lips, without end displacements of the protrusions at A and B, is proportional to σ_∞.

In order to solve this three-dimensional complicated problem the part-through crack with its particular shape was replaced by an equivalent through the thickness of the plate crack, which was submitted to a loading mode of the cracked plate, assumed to derive from the superposition of three simple loading cases indicated in Fig. 2.

Fig. 2a represents the plate with its equivalent through crack subjected to a uniform tensile stress σ_∞ at infinity, whereas Figs. 2b and 2c indicate the same plate subjected to a continuously distributed axial force ($N(x, 0)$) and moment ($M(x, 0)$) along the whole length of the crack. This distribution of forces and moments was assumed to apply at the midplane of the plate. These latter distributions of forces and moments along the length of the equivalent through crack were introduced to take care of the unsymmetric loading mode of the plate engendered by the part-through crack.

This difference in the mode of loading of the cracked plate from the respective line-spring model [**1**] was introduced to take care of the weakness of this model, which assumes that, at the front ends of the lips of the

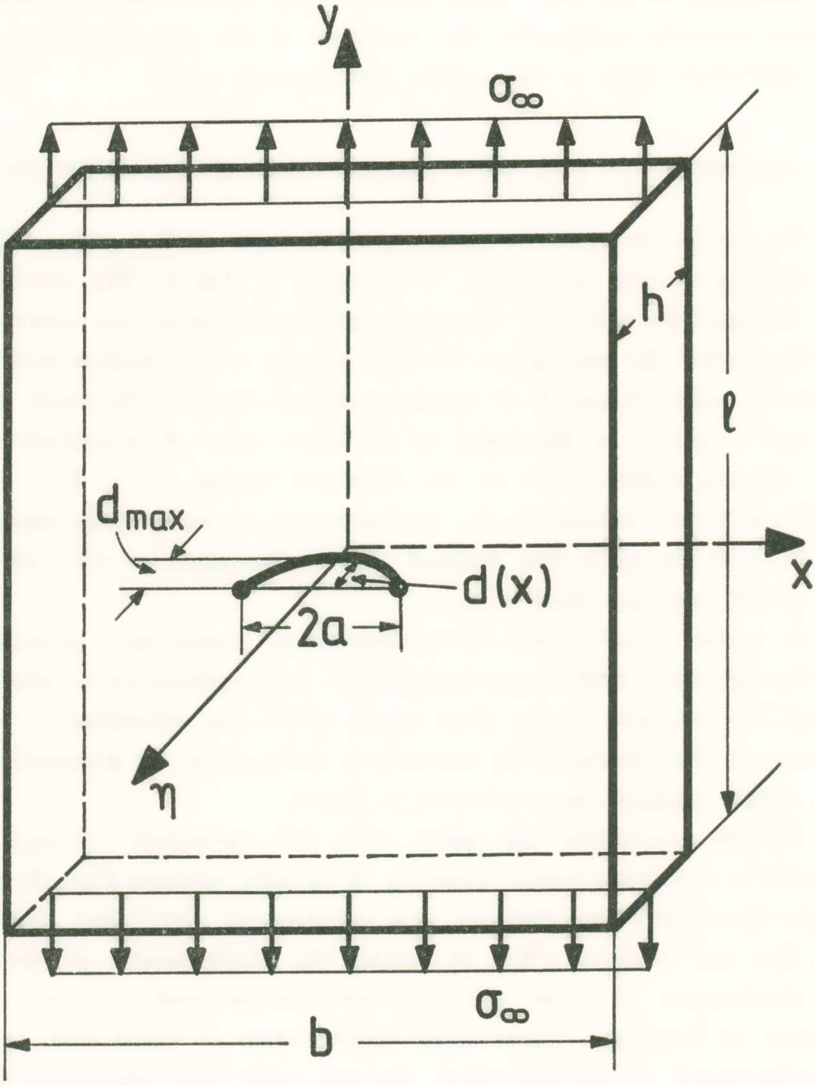

Fig. 1. A surface crack penetrating the plate thickness under uniform tension.

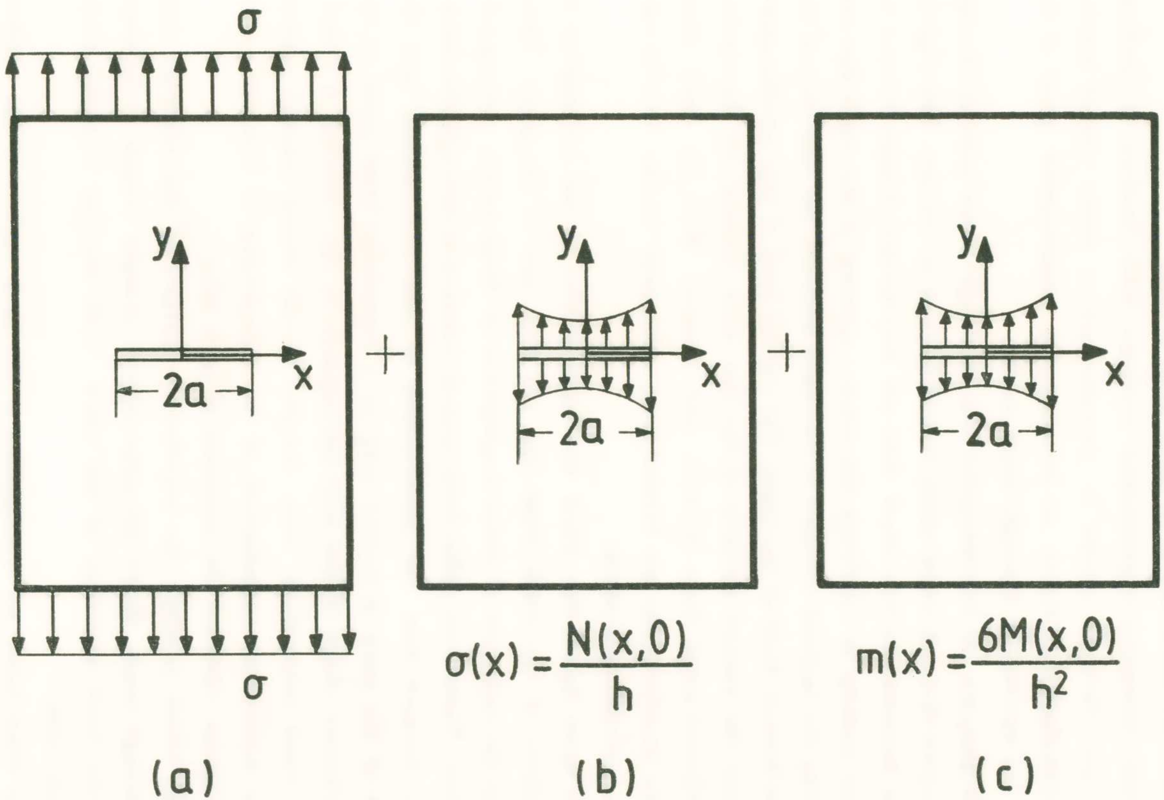

Fig. 2. The equivalent cracked plates of a surface cracked plate: a) The central cracked plate subjected to uniform tension at remote boundary. b) A continuously distributed force acts on the crack surface. c) A continuously distributed moment acts on the crack surface.

crack, where the crack intersects the near free-surface of the plate, the values of the stress intensity factor and the respective crack opening displacement are zero, since the crack depth at these ends is zero.

However, extensive experimental evidence with caustics in artificial and actual part-through cracks in plexiglas plates under overall tension (elliptic or circular) constituted an incontestable experimental proof of the validity of the equivalent through-crack model.

Fig. 3a presents the interferogram of a laser light beam passing through the lips of a part-through crack under overall tension at infinity. The slightly curved lines between the two black dots are interference fringes formed by the light rays passing in —between the crack— opening of the crack lips and reflected along the inclined surfaces of the crack between the near face of the ilate and the bottom front of the crack. The curved lines of this interferogram indicated that the warped surfaces of the lips were formed by the continuously distributed axial force $N(x, 0)$ and moment $M(x, 0)$, since these fringes of the interferogram are formed from reflections of the two lip-surfaces of the part-through crack.

In the same figure two black dots appear also at the extremities of the intersections of the crack front and the near face of the plate. These dots indicate the existence of stress singularities at these points, corresponding to caustics. These dots differ from typical caustics in through the thickness cracks, because here the phenomenon is three-dimensional and the deformation of the plate is limited only to a superficial front layer of the plate. The circular shape of the dots corresponds to the creation of a shallow hill at these extremities, since dimples should create cuspoid curves. Moreover, a meticulous examination of the topography of this area in a Taly-surf recorder certified the existence of such hills.

Fig. 3b, which presents the interference pattern of the reflected rays in a part-through crack, shows the same almost straight fringes in-between the lips of the front near-face of the crack, with the lips showing some COD at their ends.

On the other hand, an examination of the back surface of the cracked plate with transmitted light-rays revealed the creation of a shallow trough, indicated in Fig. 3c, having the shape of an ellipse, with its major axis collinear with the front trace of the crack.

All this experimental evidence suggested the necessity of introduction of the equivalent through-crack model with a loading mode indicated in Fig. 2.

The following assumptions were made in the model :

i) The thickness averaged tensile stresses σ_∞ at infinity and $\sigma(x)$ along the crack lips of the equivalent crack, as well as the nominal bending stress distributions $m(x)$ along the length of the crack are approximated by the following power functions :

$$\begin{aligned} \sigma(x) &\equiv \frac{N(x, 0)}{h} = A\left\{1 + H\left(\frac{x}{a}\right)^{2S}\right\}\sigma_\infty, \quad |x| \leqq a \\ m(x) &\equiv \frac{6M(x, 0)}{h^2} = B\left\{1 + L\left(\frac{x}{a}\right)^{2T}\right\}\sigma_\infty, \quad |x| \leqq a \end{aligned} \tag{1}$$

where A, B, H and L are unknown constants to be determined and the exponents S and T are unknown integers.

The introduction of the $\sigma(x)$- and $m(x)$-distributions expressed in relations (1) was based on considerations of constraints in the crack, which must be variable along the length of the crack, symmetric with respect to Oy-axis and therefore imposing that the exponents S and T must be integers.

ii) The three-dimensional character of the problem was approximated in the vicinity of the crack region ($|x| \leqq a$) as being piecewise plane, where the plate was assumed composed of a series of thin slices created by cuts parallel to the Oyz-plane (Fig. 4). The thicknesses of these slices were varying, so that the individual plane-strain plates with edge cracks of depth $d(x)$ may be approximated with the fronts of their cracks being normal to their lateral faces. Each of these sliced edge-cracked plates was assumed as loaded by an axial force and moment as shown in Fig. 4. The magnitudes of these forces and moments correspond to each slice located in Fig. 2. Then, the crack-face displacements of a part-through crack were related to the deformations of these individual slice strips by compliance conditions.

In this way, we adopt the same philosophy with the Rice and Levy's line-spring model [**1**], where the part-through surface crack is assumed consisting of a continuously distributed line spring with compliance-coefficients selected to match the respective compliance of the individual edge-cracked strip under conditions of plane-strain, but we modify the

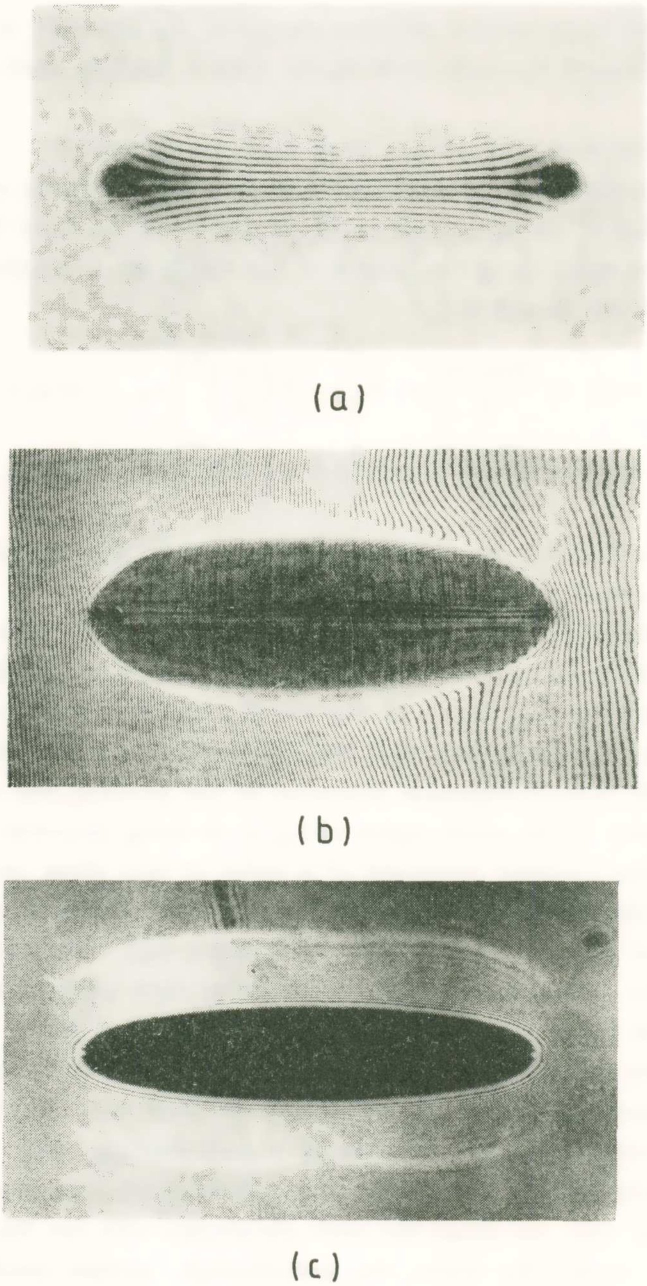

Fig. 3. a) The interferogram of a laser light beam passing through the lips of a part through-crack. b) The interference pattern of the *reflected rays in a part-through* crack. c) The interference pattern of the transmitted light rays through the part-through crack.

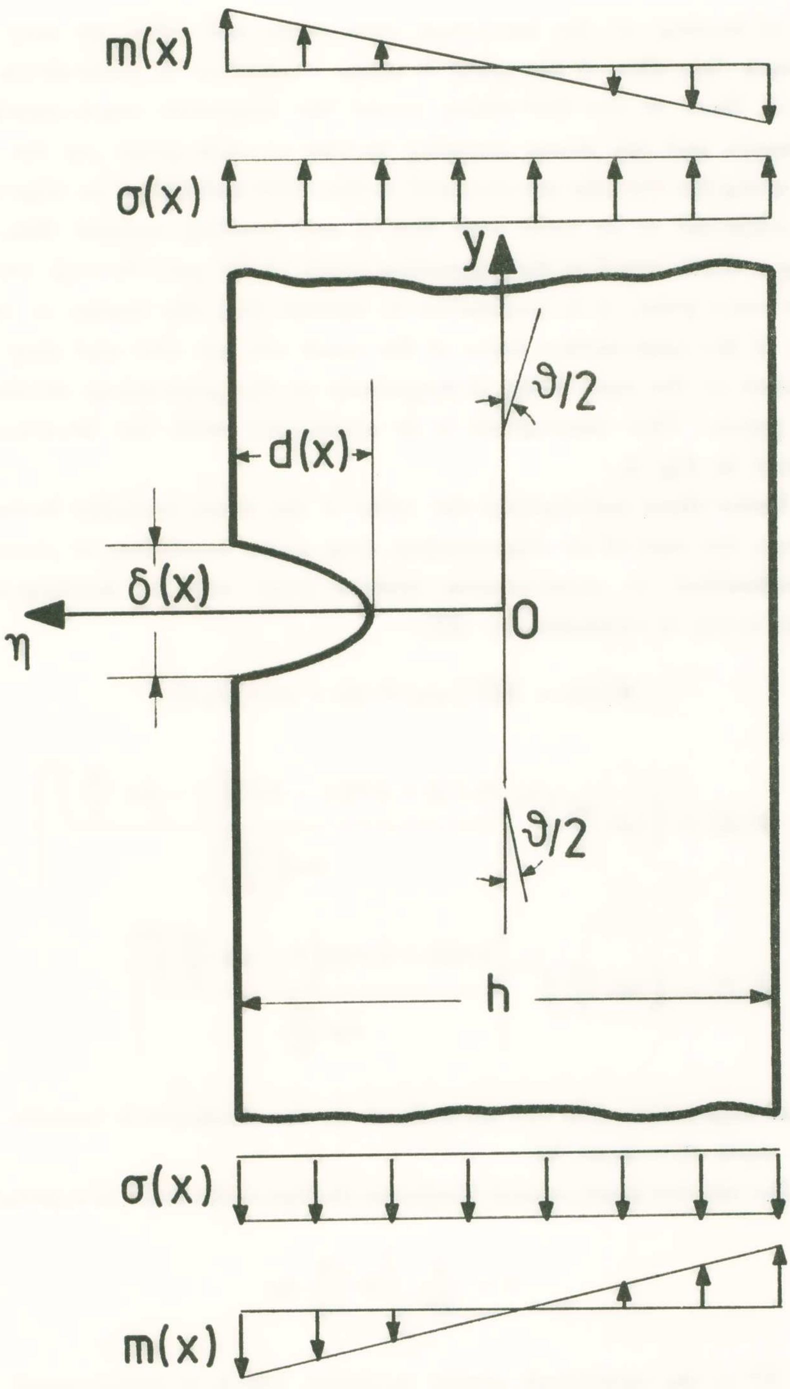

Fig. 4. An edge cracked strip subject to axial force and moment.

mode of loading of the individual slîce-strips and thus we may assume that each thin slice of the plate is under conditions of plane-stress.

iii) Since in the line-spring model the respective crack-opening displacements and the stress intensity factors at each point on the surface crack along the Ox-axis are identical to the COD and SIF of an edge-cracked strip subjected to an axial load N(x, 0) and bending moment M(x, 0) and having a depth equal to the respective depth of the part-through crack d(x) at the same point, it is imperative to assume that the depths at the end-points of the near-surface trace of the crack are not zero and they have a dimension of the same order of magnitude as the protrusions developed at these points. This assumption is in conformity with the blunting effect indicated in Fig. 3.

Under these assumptions the value of the stress intensity factor, derived from the case of an edge-cracked strip under conditions of plane strain and submitted to axial-tension stresses $\sigma(x)$ and to bending-moment stresses $m(x)$, is expressed by [**17**] :

$$K_I^e(x) = \sqrt{2h}\left\{\sigma(x)\,F_t(\xi) + m(x)\,F_b(\xi)\right\} \tag{2}$$

where :

$$F_t(\xi) = \left(\tan\frac{\pi\xi}{2}\right)^{1/2}\left\{\frac{0.752 + 2.02\,\xi + 0.37\left(1 - \sin\frac{\pi\xi}{2}\right)^3}{\cos\left(\frac{\pi\xi}{2}\right)}\right\}$$

$$F_b(\xi) = \left(\tan\frac{\pi\xi}{2}\right)^{1/2}\left\{\frac{0.923 + 0.199\left(1 - \sin\frac{\pi\xi}{2}\right)^4}{\cos\frac{\pi\xi}{2}}\right\} \tag{3}$$

In these expressions ξ is the normalized to the thickness h variable depth of the crack ($\xi = d(x)/h$).

The relative displacement δ between the lips of the crack is expressed by :

$$\delta = \frac{2}{E^*}\int_0^a K\frac{\partial K}{\partial P}\,da \tag{4}$$

where E* is the equivalent elastic modulus, which is either equal to the modulus of elasticity of the material of the plate for plane-stress conditions prevailing in the plate ($E^* = E$), or it is equal to $E^* = E/(1-\nu^2)$ for plane-strain conditions of the plate (ν is Poisson's ratio of the material).

Introducing Eq. (2) into relation (4) we obtain :

$$\delta(x) = \frac{4(1-\nu^2)h}{E}\left[\sigma(x)\,\alpha_{tt} + m(x)\,\alpha_{tb}\right] \tag{5}$$

where :

$$\alpha_{\lambda\mu} = \int_0^{\xi} F_\lambda(\xi)\,F_\mu(\xi)\,d\xi\,, \quad \lambda, \mu = t, b\,.$$

A simple formula for the displacement δ may be derived by using the empirical relations given in Ref. [**17**], that is :

$$\delta = \frac{4(1-\nu^2)h}{E}\left[\sigma(x)\,v_t(\xi) + m(x)\,v_b(\xi)\right] \tag{6}$$

where :

$$v_t(\xi) = \xi\,\frac{1.46 + 3.42\left(1-\cos\dfrac{\pi\xi}{2}\right)}{\left(\cos\dfrac{\pi\xi}{2}\right)^2} \tag{7}$$

and :

$$v_b(\xi) = \xi\left\{0.8 - 1.7\,\xi + 2.4\,\xi^2 + \frac{0.66}{(1-\xi)^2}\right\} \tag{8}$$

Introducing now relation (1) into Eqs. (6) to (8) for $x = 0$ and $\xi_0 = d/h$ ($d = d_0$ for the maximum depth of the crack) we obtain :

$$A = \frac{F_b(\xi_0)\,\dfrac{\delta(0)\,E}{4(1-\nu^2)\,\sigma_\infty h} - v_b(\xi_0)\,\dfrac{K(0)}{\sigma_\infty (2h)^{1/2}}}{F_b(\xi_0)\,v_t(\xi_0) - F_t(\xi_0)\,v_b(\xi_0)} \tag{9a}$$

$$B = \frac{v_t(\xi_0)\,\dfrac{K(0)}{\sigma_\infty (2h)^{1/2}} - F_t(\xi_0)\,\dfrac{d(0)\,E}{4(1-\nu^2)\,\sigma_\infty h}}{F_b(\xi_0)\,v_t(\xi_0) - F_t(\xi_0)\,v_b(\xi_0)} \tag{9b}$$

Moreover, for $x = a$, $\xi_a = \dfrac{d(a)}{h}$ and then we derive :

$$H = \frac{1}{A}\left\{\frac{F_b(\xi_a)\,\dfrac{\delta(a)\,E}{4(1-\nu^2)\,\sigma_\infty h} - v_b(\xi_a)\,\dfrac{K(a)}{\sigma_\infty (2h)^{1/2}}}{F_b(\xi_a)\,v_t(\xi_a) - F_t(\xi_a)\,v_b(\xi_a)}\right\} - 1 \tag{10a}$$

and :

$$L = \frac{1}{B}\left\{\frac{v_t(\xi_a)\dfrac{K(a)}{\sigma_\infty(2h)^{1/2}} - F_t(\xi_a)\dfrac{\delta(a)E}{4(1-\nu^2)\sigma_\infty h}}{F_b(\xi_a)\,v_t(\xi_a) - F_t(\xi_a)\,v_b(\xi_a)}\right\} - 1 \qquad (10b)$$

Now the unknown constants A, B, H and L in Eq. (1) are completely determined, provided that the values of the exponents T and S are defined. These values will be determined by solving the boundary-value problem of the cracked plate under the loading conditions depicted in Fig. 2.

However, it should be pointed out here that the particular values for K(x) and δ(x) at the bottom of the crack and at the intersections of the front of the crack and the near the free-face of the cracked plate were taken from empirical formulas, as they have considered also in refs. [**4**], [**17**] and [**21**, **22**] and they are only approximate. The best method to define the values of K(0) and δ(0) is by defining the crack opening displacement δ(0) at $x = 0$ from the interferograms of Fig. 3b, c and the K(0) from the interferogram of Fig. 3a, which gives the crack-tip opening displacement at the bottom of the part-through crack. Another possibility is the photoelestic method, as it was exemplified by Smith and co-workers [**23**].

SOLUTION OF THE EQUIVALENT THROUGH-CRACK MODEL

For the solution of the problem we shall use the approximate analysis of generalized plane-stress conditions and Kirchoff plate bending, similar to the treatment by Rice and Levy [**1**], to solve the two dimensional problems to which the part-through crack problem is analysed, by using the equivalent through-crack model introduced in this paper.

Following the procedure of this model we have to consider the three component-loading modes of the cracked plate and apply Muskhelishvili's complex stress function method [**25**] to each one of them.

It is well known that, according to this method, the components of stresses and displacements in plane problems are expressed in terms of two complex stress functions $\varphi(z)$ and $\chi(z)$ and their derivatives. For planestress conditions dominating in each thin slice the expressions for the stresses σ_x, σ_y and σ_{xy} and the displacements u and v are given by :

$$\begin{aligned}
(\sigma_x + \sigma_y) &= 4\,\mathrm{Re}[\varphi_t'(z)] = 2[\varphi_t'(z) + \overline{\varphi_t'(z)}] \\
(\sigma_y - \sigma_x + 2i\sigma_{xy}) &= 2[\bar{z}\varphi_t''(z) + \chi_t''(z)] \qquad (11) \\
(u + iv) &= \frac{(1+\nu)}{E}\left[\frac{3-\nu}{1-\nu}\varphi_t(z) - z\,\overline{\varphi_t(z)} - \overline{\chi_t'(z)}\right]
\end{aligned}$$

The subscript t, introduced in the complex stress functions, indicates that these relations are valid for an overall tension applied to the cracked plate. This means that these relations will be applied for the loading modes indicated in Figs. 2a and 2b. For this loading mode of the plate the boundary conditions are given by :

$$\sigma_y = \sigma_\infty \quad \sigma_{xy} = 0 \quad \text{at} \quad y \to \infty \tag{12}$$

$$\sigma_y = \frac{N(x, 0)}{h} = \sigma(x) \quad \sigma_{xy} = 0 \quad \text{at} \quad y = 0 \, |x| \leqq a \tag{13}$$

Moreover, for $y = 0$, $x > a$ the components of stresses and displacements should be continuous. Adding the boundary conditions (12) and (13) along the crack, the problem is readily reduced to a simple Hilbert problem, where we have to determine a sectionally holomorphic function $\varphi_t(z)$, which is defined all over the plate and which contains a discontinuity along the crack front. For the particular symmetric boundary conditions, existing for the tensile mode of loading, the complex stress function $\varphi_t(z)$ consists of two components. The one is derived from the loading mode appearing in Fig. 2a. For these boundary-conditions it is already well known that the stress function $\varphi'_{t_1}(z)$ is expressed by :

$$\varphi'_{t_1}(z) = -\frac{1}{2\pi}(z^2 - a^2)^{1/2} \int_{-a}^{a} \frac{\sigma_\infty (a^2 - t^2)^{1/2}}{t - z} dt$$

which yields readily that :

$$\varphi'_{t_1} = \frac{\sigma_\infty}{2}\left[\frac{z}{(z^2 - a^2)^{1/2}} - 1\right] \tag{14}$$

For the loading mode indicated in Fig. 2b we have :

$$\varphi'_{t_2}(z) = \frac{1}{2\pi}(z^2 - a^2)^{-1/2} \int_{-a}^{a} A\left[1 + H\left(\frac{t}{a}\right)^{2S}\right] \sigma_\infty \frac{(a^2 - t^2)^{1/2}}{t - z} dt$$

which, after some algebra, yields :

$$\varphi'_{t_2} \simeq -\frac{A\sigma_\infty}{2}\left[\frac{z}{(z^2 - a^2)^{1/2}} - 1\right] - \frac{AH\sigma_\infty}{\pi} \sum_{r=0}^{R} (-1)^r \frac{\frac{1}{2}\left(\frac{1}{2} - 1\right)\cdots\left(\frac{1}{2} - r + 1\right)}{r!} \times$$

$$\times \sum_{p=0}^{2,4,\ldots,P} \frac{1}{2(S+r)+p+1} \frac{z}{(z^2 - a^2)^{1/2}} \left(\frac{a}{z}\right)^{p+2}. \tag{15}$$

It can be readily shown first that the expression for φ'_{t_2} is convergent in the domain $|t| \leqq a$, since in this domain the function $(t-z)^{-1}$ converges for $(t/z) < 1$. Then, the components $(\varphi'_{t_1} + \varphi'_{t_2})$ of the complex-stress function $\varphi(z)$, taking care of the tensile mode of loading of the model, are expressed approximately by relations (14) and (15).

Similarly, for the bending-loading mode, indicated in Fig. 2c, the reduced moments m_x, m_y, m_{xy} and displacements u and v are expressed by :

$$
\begin{aligned}
m_x + m_y &= \frac{12}{h^2} D(1+\nu) \operatorname{Re}[\varphi'_b(z)] \\
m_x - m_y + i m_{xy} &= \frac{12}{h^2} D(1+\nu)[\bar{z}\varphi''_b(z) + \chi''_b(z)] \\
(u+iv) &= -\eta[\varphi_b(z) + \overline{z\varphi'_b(z)} - \overline{\chi'_b(z)}] \\
q_x - i q_y &= -4D\varphi''_b(z)
\end{aligned} \tag{16}
$$

where the nominal bending stresses m_x, m_y and m_{xy} are expressed by $m_x = 6M_x / h^2$, $m_y = 6M_y / h^2$, $m_{xy} = 6M_{xy} / h^2$ and they correspond to the stresses at the outer extreme fibers of the cracked plate, whereas $q_{x,y}$ are expressed by :

$$
q_x = \frac{\partial M_x}{\partial x} + \frac{\partial M_{xy}}{\partial y}, \qquad q_y = \frac{\partial M_{xx}}{\partial x} + \frac{\partial M_y}{\partial y}.
$$

Finally, D expresses the flexural rigidity of the plate.

The boundary conditions for this case of loading are :

$$
\begin{aligned}
&\text{i)} \quad m_y = m_\infty = 0 \qquad &&\text{and} \quad q_y + \frac{h^2}{6}\frac{\partial m_{xy}}{\partial x} = 0 \quad \text{at} \quad y \to \infty \\
&\text{ii)} \quad m_y = \frac{6M(x,0)}{h^2} = m(x) \qquad && q_y + \frac{h^2}{6}\frac{\partial m_{xy}}{\partial x} = 0 \quad \text{at} \quad y = 0 \; |x| \leqq a
\end{aligned} \tag{17}
$$

Proceeding in a similar way, as in the previous case, we obtain for the component of bending of the plate the relation :

$$
-\frac{(3+\nu)Eh}{2(1-\nu^2)} \varphi'_b(z) = \frac{1}{2\pi}(z^2 - a^2)^{-1/2} \int_{-a}^{a} B\left[1 + L\left(\frac{t}{a}\right)^{2T}\right] \sigma_\infty \frac{(a^2 - t^2)^{1/2}}{t - z}\, dt
$$

which, after some algebra, yields :

$$\frac{(3+\nu)\,Eh}{2\,(1-\nu^2)}\,\varphi_b'(z) \simeq \frac{B\sigma_\infty}{2}\left[1-\frac{z}{(z^2-a^2)^{1/2}}\right]+$$
$$+\frac{BL\sigma_\infty}{\pi}\sum_{r=0}^{R}(-1)^r\,\frac{\frac{1}{2}\left(\frac{1}{2}-1\right)\ldots\left(\frac{1}{2}-r+1\right)}{r!}\times \tag{18}$$
$$\times\sum_{p=0}^{2,4,6,\ldots,P}\frac{1}{2\,(T+r)+p+1}\;\frac{z}{(z^2-a^2)^{1/2}}\left(\frac{a}{z}\right)^{p+2}.$$

Again, we can readily show the convergence of the relation (18) in the domain, $|x| \leqq a$ enclosing the part-through crack.

Expressions (14), (15) and (18) allow the evaluation of the stress and displacement fields around the part-through crack and the determination of the stress intensity factor at the crack front.

THE EVALUATION OF THE STRESS AND DISPLACEMENT FIELDS

The problem of a part-through crack along the Ox-axis ($y=0$) in an infinite plate subjected to tensile stresses σ_∞ at infinity presents a geometric and loading symmetry and therefore only the mode-I stress intensity factor is operative. For convenience we introduce Westergaard's complex stress-function $Z_1(z)$, which yields the following components for the stresses and displacements for each thin slice :

i) For the stresses:

$$\begin{aligned}\sigma_x &= \mathrm{Re}Z_1 - y\,\mathrm{Im}Z_1' \\ \sigma_y &= \mathrm{Re}Z_1 + y\,\mathrm{Im}Z_1' \\ \sigma_{xy} &= -y\,\mathrm{Re}Z_1'\end{aligned} \tag{19}$$

ii) For the displacements (in the case of plane-stress conditions):

$$\begin{aligned}u &= \frac{1}{E}\left\{(1-\nu)\,\mathrm{Re}\bar{Z}_1-(1+\nu)\,y\,\mathrm{Im}Z_1\right\} \\ v &= \frac{1}{E}\left\{2\,\mathrm{Im}\bar{Z}_1-(1+\nu)\,y\,\mathrm{Re}Z_1\right\} \\ w &= -\frac{\nu}{E}\int(\sigma_x+\sigma_y)\,d\eta\end{aligned} \tag{20}$$

iii) For plane-strain conditions the components of displacement are given by:

$$u = \frac{(1+\nu)}{E}\left\{(1-2\nu)\,\mathrm{Re}\bar{Z}_1 - y\,\mathrm{Im}Z_1\right\}$$

$$v = \frac{(1+\nu)}{E}\left\{2(1-2\nu)\,\mathrm{Im}\bar{Z}_1 - y\,\mathrm{Re}Z_1\right\} \tag{21}$$

$$w = 0$$

The complex stress function $Z_1(z)$ can be expressed in terms of the functions $\varphi'_{t_1}(z)$, $\varphi'_{t_2}(z)$ and $\varphi'_b(z)$ and it is given by:

$$Z_1(z) = \sigma_\infty (1-A-B)\frac{z}{(z^2-a^2)^{1/2}} -$$

$$-\frac{2AH\sigma_\infty}{\pi}\sum_{r=0}^{R}(-1)^r\frac{\frac{1}{2}\left(\frac{1}{2}-1\right)\cdots\left(\frac{1}{2}-r+1\right)}{r!}\sum_{p=0}^{2,4,6,\ldots,P}\frac{1}{2(S+r)+p+1}$$

$$\left(\frac{a}{z}\right)^p\frac{z}{(z^2-a^2)^{1/2}} - \tag{22}$$

$$-\frac{2BL\sigma_\infty}{\pi}\sum_{r=0}^{R}(-1)^r\frac{\frac{1}{2}\left(\frac{1}{2}-1\right)\cdots\left(\frac{1}{2}-r+1\right)}{r!}\sum_{p=0}^{2,4,6,\ldots,P}\frac{1}{2(T+r)+p+1}$$

$$\left(\frac{a}{z}\right)^p\frac{z}{(z^2-a^2)^{1/2}}$$

In order to evaluate the stress intensity factor at the crack front, it is advisable to introduce the transformation:

$$\zeta = (z-a) \tag{23}$$

and Eq. (22) becomes:

$$Z_1(\zeta) = \sigma_\infty (1-A-B) \frac{\zeta + a}{[(\zeta+2a)\zeta]^{1/2}} -$$

$$- \frac{2AH\sigma_\infty}{\pi} \sum_{r=0}^{R} (-1)^r \frac{\frac{1}{2}\left(\frac{1}{2}-1\right)\cdots\left(\frac{1}{2}-r+1\right)}{r!}$$

$$\sum_{p=0}^{2,4,6,\ldots,P} \frac{1}{2(S+r)+p+1} \left(\frac{a}{\zeta+a}\right)^{p+2} \frac{\zeta+a}{[(\zeta+2a)\zeta]^{1/2}} - \tag{24}$$

$$- \frac{2BL\sigma_\infty}{\pi} \sum_{r=0}^{R} (-1)^r \frac{\frac{1}{2}\left(\frac{1}{2}-1\right)\cdots\left(\frac{1}{2}-r+1\right)}{r!}$$

$$\sum_{p=0}^{2,4,6,\ldots,P} \frac{1}{2(T+r)+p+1} \left(\frac{a}{\zeta+a}\right)^{p+2} \frac{\zeta+a}{[(\zeta+2a)\zeta]^{1/2}}$$

Considering the fact, that as $|\zeta| \to 0$, the quantity $Z_1(\zeta)(\zeta)^{1/2}$ tends to a constant value, we define the stress intensity factor K_I^s as :

$$K_I^s = \sqrt{2\pi} \lim_{\zeta \to 0} [\zeta^{1/2} Z_1(\zeta)] \tag{25}$$

and this quantity, according to relation (24), is expressed by :

$$K_I^s = (K_{It}^s + K_{Ib}^s) = \left\{1 - A - \frac{2AH}{\pi} \sum_{r=0}^{R} (-1)^r \frac{\frac{1}{2}\left(\frac{1}{2}-1\right)\cdots\left(\frac{1}{2}-r+1\right)}{r!} \sum_{p=0}^{2,4,6,\ldots,P} \frac{1}{1(S+2)+p+1}\right\}$$

$$\sigma_\infty (\pi a)^{1/2} + \left\{-B \frac{2BL}{\pi} \sum_{r=0}^{R} (-1)^r \frac{\frac{1}{2}\left(\frac{1}{2}-1\right)\cdots\left(\frac{1}{2}-r+1\right)}{r!} \sum_{p=0}^{2,4,6,\ldots,P} \frac{1}{2(T+r)+p+1}\right\} \sigma_\infty (\pi a)^{1/2} \tag{26}$$

In order to define to components of stresses and displacements, we express the complex coordinate ζ in terms of the polar coordinates r, θ. We have :

$$Z_1(\zeta) = \frac{K_I^s}{(2\pi\zeta)^{1/2}} = \frac{K_I^s}{(2\pi r)^{1/2}} \left(\cos\frac{\theta}{2} - i\sin\frac{\theta}{2}\right) \tag{27}$$

Then,

$$\frac{dZ_1(\zeta)}{d\zeta} = - \frac{K_I^s}{2(2\pi)^{1/2}} \frac{1}{r^{3/2}} \left(\cos\frac{3\theta}{2} - i\sin\frac{3\theta}{2}\right) \tag{28}$$

Substituting Eqs. (27) and (28) into Eqs. (19) to (21) and considering that $y = r\sin\theta$, we derive the components of stresses and displacements for the surface part-through crack at the vicinity of the ends $|x| = a$ and $y = 0$ given by :

$$\left.\begin{matrix}\sigma_x \\ \sigma_y \\ \sigma_{xy}\end{matrix}\right\} = \frac{K_I^s}{(2\pi r)^{1/2}} \cos\frac{\theta}{2} \left\{\begin{matrix}\left[1 - \sin\frac{\theta}{2}\sin\frac{3\theta}{2}\right] \\ \left[1 + \sin\frac{\theta}{2}\sin\frac{3\theta}{2}\right] \\ \sin\frac{\theta}{2}\cos\frac{3\theta}{2}\end{matrix}\right\} \tag{29}$$

$$\sigma_\eta = 0$$

$$\left.\begin{matrix}u \\ v\end{matrix}\right\} = \frac{K_I^s}{4(2\pi)^{1/2} G} r^{1/2} \left\{\begin{matrix}\left[\frac{5-3\nu}{1+\nu}\cos\frac{\theta}{2} - \cos\frac{3\theta}{2}\right] \\ \left[\frac{7-\nu}{1+\nu}\sin\frac{\theta}{2} - \sin\frac{3\theta}{2}\right]\end{matrix}\right\} \tag{30}$$

$$w = \mp \int_0^{\pm h/2} \left[\frac{\nu}{E}(\sigma_x + \sigma_y)_t + \frac{2(\sigma_x + \sigma_y)_b\,\eta}{h}\right] d\eta$$

In the neighbourhood of the region $|x| < a$ and $y \to 0$, when plane-strain conditions prevail, we have :

$$\sigma_x = \nu(\sigma_y + \sigma_z)$$

$$\left.\begin{matrix}\sigma_y \\ \sigma_z \\ \sigma_{yz}\end{matrix}\right\} = \frac{K_I^e}{(2\pi r)^{1/2}} \cos\frac{\theta}{2} \left\{\begin{matrix}\left[1 - \sin\frac{\theta}{2}\sin\frac{3\theta}{2}\right] \\ \left[1 + \sin\frac{\theta}{2}\sin\frac{3\theta}{2}\right] \\ \sin\frac{\theta}{2}\cos\frac{3\theta}{2}\end{matrix}\right\} \tag{31}$$

and

$$u = 0$$

$$\left.\begin{matrix}v \\ w\end{matrix}\right\} = \frac{K_I^e}{4(2\pi)^{1/2} G} (r)^{1/2} \left\{\begin{matrix}\left[(5-8\nu)\cos\frac{\theta}{2} - \cos\frac{3\theta}{2}\right] \\ \left[(7-8\nu)\sin\frac{\theta}{2} - \sin\frac{3\theta}{2}\right]\end{matrix}\right\} \tag{32}$$

For the whole plate the complex stress function $Z_1(z)$ (Eq. (24)) yields, by introducing the transformations:

$(z - a) = r_1 e^{i\vartheta_1}$ and $(z + a) = r_2 e^{i\vartheta_2}$:

$$Z_1(z) = \sigma_\infty [1-A-B] \frac{r}{(r_1 r_2)^{1/2}} e^{i\left(\vartheta - \frac{\vartheta_1+\vartheta_2}{2}\right)} -$$

$$- \frac{2AH\sigma_\infty}{\pi} \sum_{r=0}^{R} (-1)^r \frac{\frac{1}{2}\left(\frac{1}{2}-1\right)\dots\left(\frac{1}{2}-r+1\right)}{r!}$$

$$\sum_{p=0}^{2,4,6,..,P} \frac{1}{2(S+r)+p+1} \frac{r}{(r_1 r_2)^{1/2}} \left(\frac{a}{r}\right)^{p+2} e^{-i\left[(p+1)\vartheta + \frac{\vartheta_1+\vartheta_2}{2}\right]} - \tag{33}$$

$$- \frac{2BL\sigma_\infty}{\pi} \sum_{r=0}^{R} (-1)^r \frac{\frac{1}{2}\left(\frac{1}{2}-1\right)\dots\left(\frac{1}{2}-r+1\right)}{r!} \sum_{p=0}^{2,4,6,..,P} \frac{1}{2(T+r)+p+1} \frac{r}{(r_1 r_2)^{1/2}}$$

$$\left(\frac{a}{r}\right)^{p+2} e^{-i\left[(p+1)\vartheta + \frac{\vartheta_1+\vartheta_2}{2}\right]}$$

and

$$Z_1'(z) = -\sigma_\infty [1-A-B] \frac{a^2}{(r_1 r_2)^{3/2}} e^{-i\left[\frac{3}{2}(\vartheta_1+\vartheta_2)\right]} +$$

$$+ \frac{2AH}{\pi} \sum_{r=0}^{R} (-1)^r \frac{\frac{1}{2}\left(\frac{1}{2}-1\right)\dots\left(\frac{1}{2}-r+1\right)}{r!}$$

$$\sum_{p=0}^{2,4,6,..,P} \frac{1}{2(S+r)+p+1} \left\{ \frac{p+2}{(r_1 r_2)^{1/2}} \left(\frac{a}{r}\right)^{p+2} e^{-i\left[(p+2)\vartheta + \frac{\vartheta_1+\vartheta_2}{2}\right]} + \right.$$

$$\left. + \frac{a^2}{(r_1 r_2)^{3/2}} \left(\frac{a}{r}\right)^{p+2} e^{-i\left[(p+2)\vartheta + \frac{3(\vartheta_1+\vartheta_2)}{2}\right]} \right\} + \tag{34}$$

$$+ \frac{2BL}{\pi} \sum_{r=0}^{R} (-1)^r \frac{\frac{1}{2}\left(\frac{1}{2}-1\right)\dots\left(\frac{1}{2}-r+1\right)}{r!}$$

$$\sum_{p=0}^{2,4,6,..,P} \frac{1}{2(T+r)+p+1} \left\{ \frac{p+2}{(r_1 r_2)^{1/2}} \left(\frac{a}{r}\right)^{p+2} e^{-i\left[(p+1)\vartheta + \frac{\vartheta_1+\vartheta_2}{2}\right]} + \right.$$

$$\left. + \frac{a^2}{(r_1 r_2)^{3/2}} \left(\frac{a}{r}\right)^{p+2} e^{-i\left[(p+1)\vartheta + \frac{3(\vartheta_1+\vartheta_2)}{2}\right]} \right\}$$

$$
\begin{aligned}
\overline{Z_1(z)} = {} & \sigma_\infty [1-A-B] (r_1 r_2)^{1/2} e^{i\left(\frac{\vartheta_1+\vartheta_2}{2}\right)} - \\
& - \frac{2AH\sigma_\infty}{\pi} \sum_{r=0}^{R} (-1)^r \frac{\frac{1}{2}\left(\frac{1}{2}-1\right)\dots\left(\frac{1}{2}-r+1\right)}{r!} \sum_{p=0}^{2,4,6,..,P} \frac{1}{2(S+r)+p+1} \\
& \left\{ \sum_{q=1}^{(p-2)/1} \frac{1}{p-2q-1} \prod_{q=1}^{(p-2)/2} \frac{(p-2q+1)}{(p-2q)} \left| (r_1 r_2)^{1/2} \left(\frac{a}{r}\right)^{p-2q} e^{i\left[\frac{\vartheta_1+\vartheta_2}{2} - (p-2q)\vartheta\right]} + \frac{1}{a} \sec^{-1}\left(\frac{r}{a} e^{i\vartheta}\right) \right| \right\} - \qquad (35) \\
& - \frac{2BL\sigma_\infty}{\pi} \sum_{r=0}^{R} (-1)^r \frac{\frac{1}{2}\left(\frac{1}{2}-1\right)\dots\left(\frac{1}{2}-r+1\right)}{r!} \sum_{p=0}^{2,4,6,..,P} \frac{1}{2(T+r)+p+1} \\
& \left\{ \sum_{q=1}^{(p-2)/2} \frac{1}{p-2q-1} \prod_{q=1}^{p-2q+1} \left| (r_1 r_1)^{1/2} \left(\frac{a}{r}\right)^{p-2q} e^{i\,(\vartheta_1+\vartheta_2)/2-(p-2q)\vartheta]} + \frac{1}{a} \sec^{-1}\left(\frac{r}{a} e^{i\vartheta}\right) \right| \right\}
\end{aligned}
$$

Substituting relations (33) to (35) into Eqs. (19) and (20) we obtain the values for stresses and displacements in everyone of the slices corresponding to the part-through crack section of the plate.

DETERMINATION OF THE EXPONENTS S AND T

It remains only to define the values of the exponents S and T in relations (1). It should be mentioned at once that, due to the form of Eqs. (1), the extremities of each of the curves $\sigma(x) = f(x)$ and $m(x) = \varphi(x)$ along the crack length, that is for $x = 0$ and $|x| = a$, are independent of the values of the exponents S and T. They depend only on the values of constants A and B for the point $x = 0$ and on the products AH and BL for the extremities $|x| = a$. Only the slopes of the curves $\sigma(x)$ and $m(x)$ depend on the values of the exponents S and T.

Moreover, it is worthwhile indicating that for the line-spring model the assumption at the front ends of the crack, that the crack opening displacement and the respective stress intensity factor there are zero, is of no importance from the point of view of computing the value of the stress intensity factor at the bottom of the crack front by the numerical solution of the respective integral equation, because it may be readily shown that for non-zero values of these quantities a constant of integration should be added in the solution of the integral equation, which does not influence the value of SIF at least at the vicinity of the deepest point of the part-through crack.

On the contrary, in our equivalent through-crack model the importance of the accurate evaluation of these quantities is primordial, since they contribute mainly to the accurate evaluation of the various constants of the solution.

In order to define the values of the exponents N and M we can write Eq. (26) in the form :

$$(1-A-B)-\frac{2AH}{\pi}\sum_{r=0}^{R}(-1)^r\frac{\frac{1}{2}\left(\frac{1}{2}-1\right)\cdots\left(\frac{1}{2}-r+1\right)}{r!}\sum_{p=0}^{2,4,6,\ldots,P}\frac{1}{2(S+r)+p+1}-$$
$$-\frac{2BL}{\pi}\sum_{r=0}^{R}(-1)^r\frac{\frac{1}{2}\left(\frac{1}{2}-1\right)\cdots\left(\frac{1}{2}-r+1\right)}{r!}\sum_{p=0}^{R}\frac{1}{2(T+r)+p+1}=\frac{K_I^s(\xi)}{\sigma_\infty(\pi a)^{1/2}} \tag{36}$$

and apply it at the extremities of the crack front for which $|x| = a$. If we introduce the quantities :

$$A_0 = (1-A-B)\,, \qquad B_0 = \frac{K_I^s(\xi_a)}{\sigma_\infty(\pi a)^{1/2}}$$

$$f(S) = \sum_{r=0}^{R}(-1)^r\frac{\frac{1}{2}\left(\frac{1}{2}-1\right)\cdots\left(\frac{1}{2}-r+1\right)}{r!}\sum_{p=0}^{2,4,6,\ldots,P}\frac{1}{2(S+r)+p+1}$$

$$f(T) = \sum_{r=0}^{R}(-1)^r\frac{\frac{1}{2}\left(\frac{1}{2}-1\right)\cdots\left(\frac{1}{2}-r+1\right)}{r!}\sum_{p=0}^{2,4,6,\ldots,P}\frac{1}{2(T+r)+p+1}$$

and insert these values into Eq. (36), we obtain,

$$f(T)-\left[A_0-B_0-\frac{2AH}{\pi}f(S)\right]\frac{\pi}{2BL}=0 \tag{37}$$

Since the exponents T and S must be integers, Eq. (37) will yield the optimum combination for the integer values of T_i and S_j when the difference between $f(T_i)$ and

$$\left[A_0 - B_0 - \frac{2AH}{\pi} f(S_j)\right] \frac{\pi}{2BL} \text{ is minimized, that is :}$$

$$\left[f(T_i) - \left[A_0 - B_0 - \frac{2AH}{\pi} f(S_j)\right] \frac{\pi}{2BL}\right] \rightarrow \text{minimum} \tag{38}$$

for some pair of values for T_i *and* S_j *running between unity and infinity.* In practical calculations these exponents depend on the values of the stress intensity factor at the botton $(x = 0)$ and the extremities $(|x| = a)$ of the elliptic part-through crack.

Next we define the value of the stress intensity factor K_I^s at $|x| = a$ from either Irwin's formula [**2**], or any other approximate relation [**7**], or from a convenient experimental procedure [**23**, **24**]. As soon as the accurate value of K^1 at $|x| = a$ is determined we can proceed numerically to find the minimum of the expression of relation (38).

RESULTS AND DISCUSSION

In order to show the potentialities of the method at least for the evaluation of the variation of the stress intensity factor along the front of the part-through elliptic crack, we applied the model to some particular concrete problem. The problem considered was of a thin plate, containing a part-through elliptic crack with $d_0/R = 0.5$ and $d_0/a = 0.2$, where d_0 is the maximum depth of the part-through elliptic crack, h is the thickness of the plate and a is the half-length of the crack at the front face of the plate.

The particular values k(0), k(a), $\delta(0)$ and $\delta(a)$ in Eqs. (9) and (10) can be evaluated from refs. [**21**] and [**26**], [**27**] and they are given by :

$$K_I^c(0) = M_0 \sigma_\infty (\pi d_0 / Q)^{1/2} \tag{39}$$

$$K_I^c(a) = M_a \sigma_\infty (\pi d_0 / Q)^{1/2} \tag{40}$$

$$\delta(0) = \frac{2(1-\nu^2) a\sigma_\infty}{E} \left[1 + \left(\frac{d_0/a}{\Phi}\right)\right] \alpha \tag{41}$$

$$\delta(a) = \beta \frac{[K_I(a)]^2}{\sigma_0 E} \tag{42}$$

where M_0 and M_a are the so-called magnification factors [**8 - 10**], which can be evaluated as discussed before. The constants α and β represent, the first, a *shape factor*, which varies between $2\left[1+\left(\frac{d_0/a}{\Phi}\right)\right]^{-1}$ and $\left[1+\left(\frac{d_0/a}{\Phi}\right)\right]^{-1}$, as it has been discussed in ref. [**21**], and the second a *singularity-correction factor*, which varies between 0.38 and unity, as it is given in refs. [**26**] and [**27**]. For our case we have chosen $\alpha = 1$ and $\beta = \pi/8$. Moreover, σ_0 is the stress at infinity corresponding to the caustics at A and B, and Φ and Q correction factor sintroduced by refs. [**8 - 10**], [**21**] and [**30**].

In our model we have assumed that the thickness-variation at the neighbourhood of the end-points of the crack is not zero, fact which was confirmed by experience with caustics, and forms a small shallow hill (see Fig. 3a). It is reasonable to accept that this hill-like zone has a size of the same order of magnitude of the plastic zones developed at the ends of the front-lips of the crack. The thickness variation at the ends of the crack front are given by :

$$\frac{d\,(a)}{h} = \frac{d_0}{h}\left[1-\left(1+\frac{r_0}{a}\right)^{-2}\right]^{1/2} \tag{43}$$

where r_0 is the radius of the unitial curve creating the caustic at the extremities of the crack-front face and evaluated by assuming equivalent plane-stress conditions for the weak-singularities at these points.

Then, the unknown quantities may be readily evaluated and thî are given as :

$$A = 0.10823, \; B = 0.76557, \; H = 83.93098 \text{ and } L = -13.39506$$

Moreover, for a number of terms in the truncated series $R = 30$ and $P = 50$, the exponents T and S can be approximately defined from Eq. (38) and they take the values :

$$T = 21 \text{ and } S = 20$$

From these values the variation of the normalized stresses $\sigma(x)/\sigma_\infty$ and $m(x)/\sigma_\infty$ can be evaluated and they are plotted in Fig. 5, whereas the values of the normalized stress intensity factor $k(x)/\sigma_\infty\left(\frac{\pi d_0}{Q}\right)^{1/2}$ along the whole crack front may readily be derived and they are traced in Fig. 6.

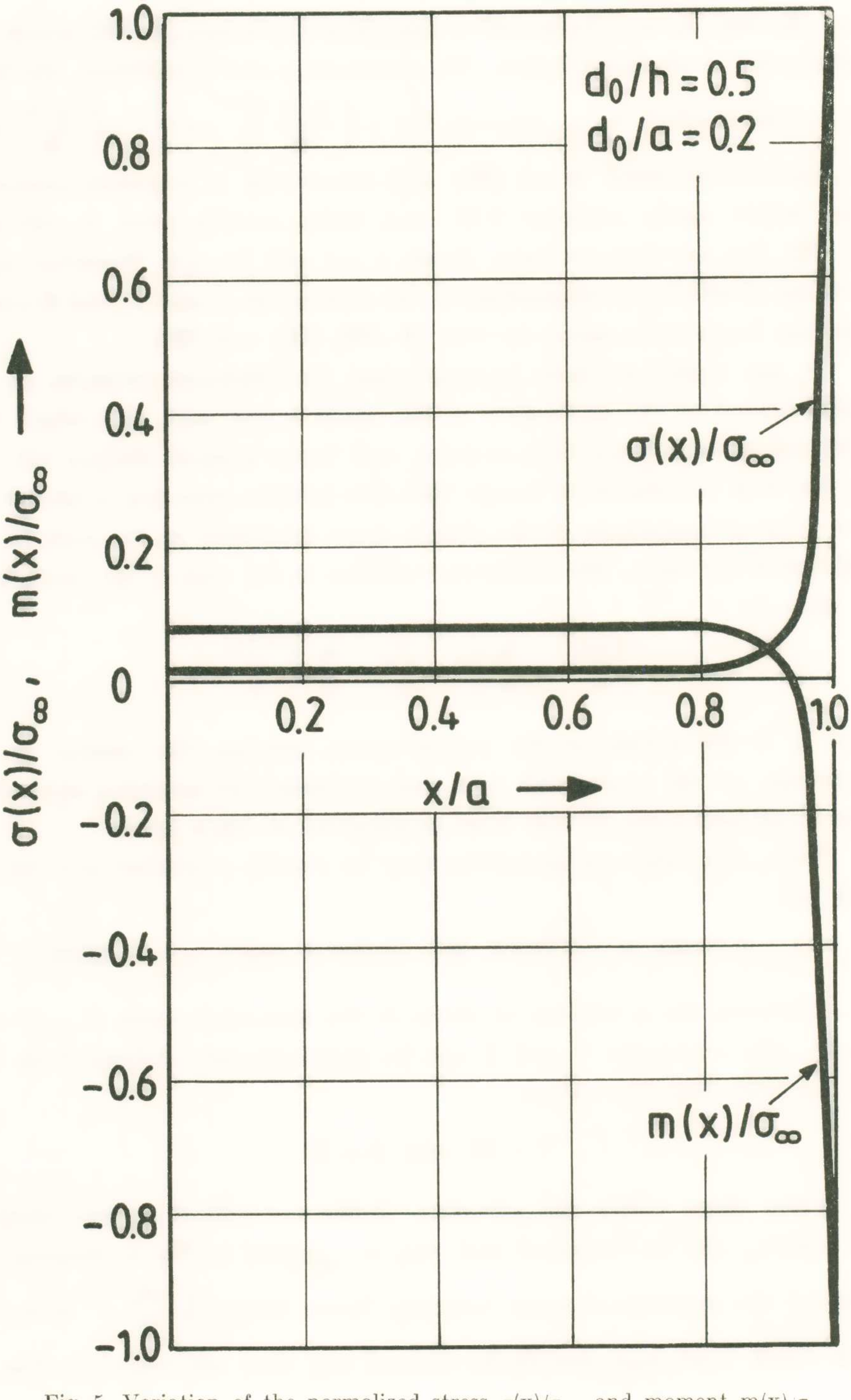

Fig. 5. Variation of the normalized stress $\sigma(x)/\sigma_\infty$ and moment $m(x)/\sigma_\infty$ along the crack-axis.

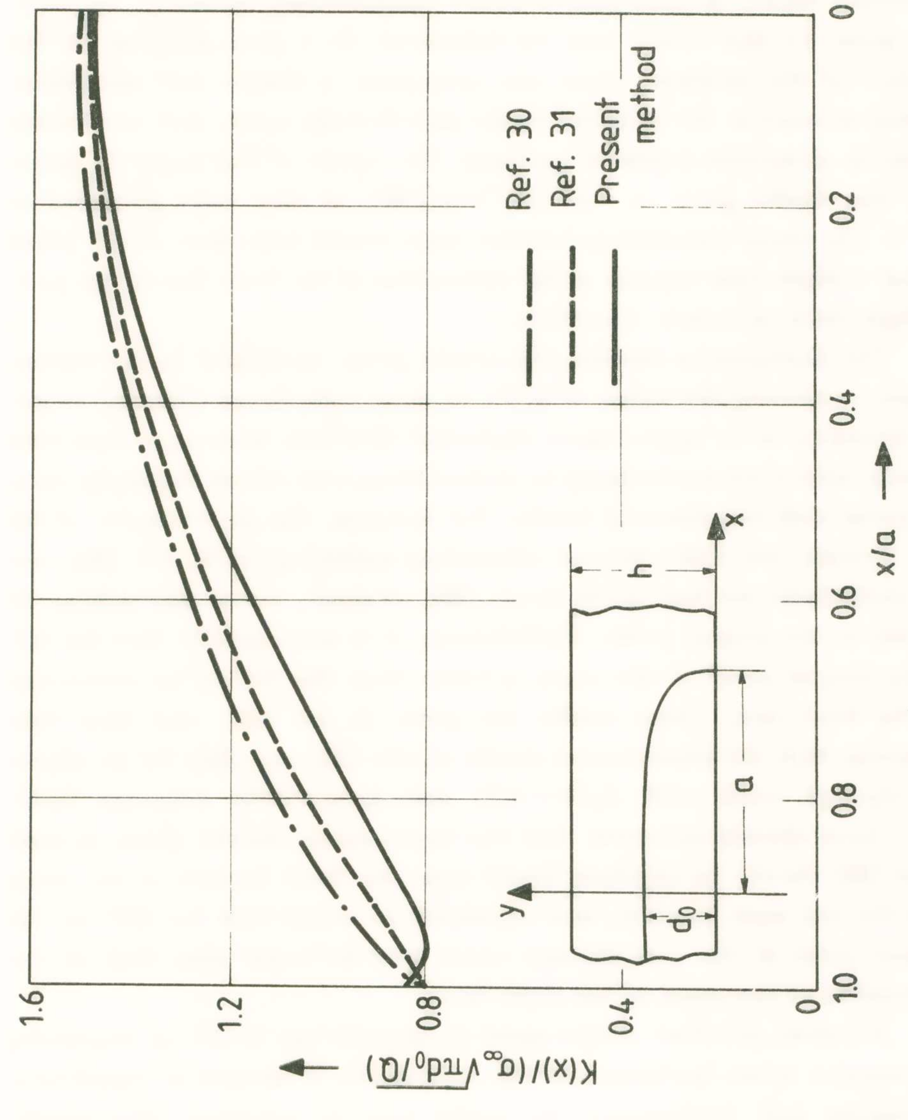

Fig. 6. Variation of stress intensity factor along the boundary of the crack.

If one considers the fact that up-to-now a closed-form solution of the problem of a part-through crack is as yet missing and the existing approximate solutions either require large amounts of computer time, as mentioned before, or yield results within unsatisfactory accuracy, the solution given by this model may be considered as a good progress to the solution of the problem, since not only gives a simple and convenient method to analyse the problem of the part-through crack, but also results within an acceptable degree of accuracy. The results of this paper fit better with the results given in refs. [**30**] and [**31**], as they have presented in Fig. 6. The major discrepancy between these results and those of this paper is that a slight knee appears at the extremities of the front lips of the part-through crack at values $x/a \simeq 0.95$.

The discrepancies between the results given up-to-now in the various papers, concerning the values of SIF's, as these were found either by empirical formulas, or by approximate numerical solutions, were sometimes very obvious, with some results being in contradiction with others, especially when compared with experimental results. For instance, the discrepancies of the SIF between the finite-element alternating method given in ref. [**28**] and the photoelastic method, given in ref. [**22**], attained values appoaching 24 percent at the deepest point. Furthermore, it is unacceptable that the SIF at the deepest point of the crack is lower than the SIF at its extremities on the front face. These results are given in ref. [**28**], and they were compared with the experimental results of refs. [**21**] and [**23**], for an elliptic part-through crack with $d_0/h = 0.75$ and $d_0/a = 0.50$. Although Smith et al. have already indicated that the experimental results given in their paper [**23**] should be somehow lower near the front surface of the crack than the real ones, however, it is impossible to accept that the SIF at the deepest point of the part-through crack may be lower than that at the extremities of the crack at the front face.

However, an effort is now spent to improve the model by expressing the complex stress functions and the components of stresses in closed-form expressions and, furthermore, the model may be combined with experimental measurements from caustics created either in the front, or the rear face of the plate, or along the internal front of the part-through crack, which will yield accurate and reliable results for the values of the unknown coef-

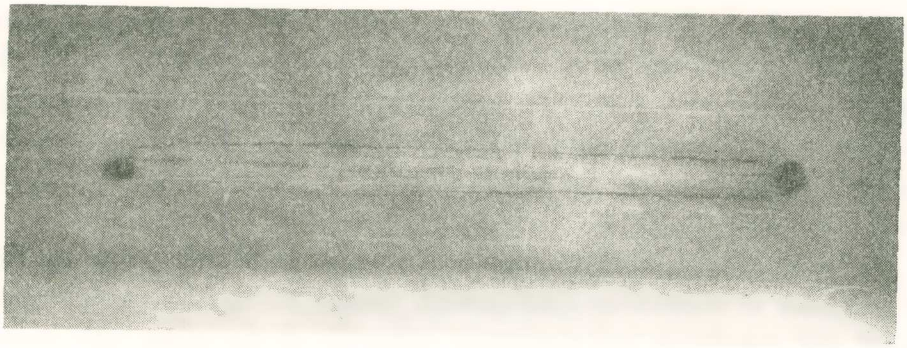

(a)

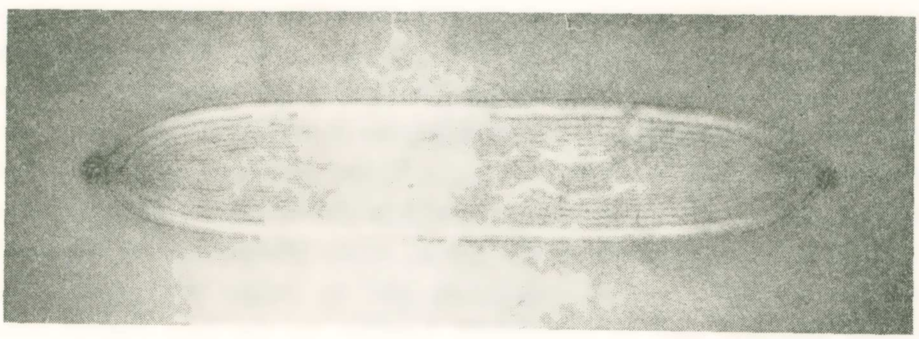

(b)

Fig. 7. Interferograms of a laser light beam passing through the part-through crack.

ficients. In this way the combined model solution with the experimental values shall constitute a completely independent method.

Indeed, the non-zero elevations at the end-points of the front-configuration of the part-through crack are directly related with the singular behavior of the stresses in this region, which is intimately related with the regional caustic created at these extremities and it is exemplified in Figs. 3a and 3b. Moreover, the COD of the crack front can be readily evaluated by the interferogram and the pseudocaustic of Fig. 7a and 7b and this will yield the values of SIF at $\varphi = 0^0$ and other angles.

Finally, it should be emphasized that the complexity in the solution of problems of internal or part-through cracks due to their three-dimensional and sometimes non-symmetric character of the stress field creates considerable difficulties in the analysis of the stress field along the crack front and especially along a boundary layer close to the plate lateral faces where the state of stress is rapidly varying and as yet unknown. Therefore due to this also fact numerical solutions at these zones are always in question as this has been clearly emphasized by Sih [32, 33]. According to this analysis the SIF and the state of stress become functions depending on the thickness-coordinate and they are rapidly diminishing along two boundary layers close to the free faces of the plate. In these zones the SIF diminishes rapidly and it takes values much smaller than those corresponding to the generalized plane-stress case. This fact implies to conjecture that the three-dimensional and non-symmetric character of the part-through crack should be considered in the solution and especially in the vicinity of the end-points of the front configuration of the crack, where plane-stress or Kirchkoff or Reissner plate bending conditions are no longer warranted. This peculiar situation may be successfully handled by the data derived from caustics which then will improve significantly the accuracy and reliability of the results derived from the model.

ΠΕΡΙΛΗΨΙΣ

Τὸ τριδιάστατον πρόβλημα τῆς ἐπιφανειακῆς μερικῆς ρωγμῆς εἰς παχεῖαν πλάκα δύναται νὰ ἀναχθῇ εἰς διδιάστατον πρόβλημα διὰ τῆς εἰσαγωγῆς τοῦ ὁμοιώματος τῆς ἰσοδυνάμου διαμπεροῦς ρωγμῆς φορτιζομένης διὰ καταλλήλου διανομῆς ἐφελκυστικῶν καὶ καμπτικῶν τάσεων κατὰ μῆκος τῶν χειλέων τῆς ρωγμῆς.

Ἡ ἀρχὴ τοῦ ὁμοιώματος βασίζεται εἰς σχετικὴν πρότασιν, γενομένην τελευταίως ὑπὸ τοῦ καθηγητοῦ J. Rice τοῦ Πανεπιστημίου Brown τῶν Η.Π.Α. καὶ τοῦ συνεργάτου του N. Levy τὸ 1972. Συμφώνως πρὸς τὸ ὁμοίωμα τοῦ Rice, τὸ ὁποῖον καὶ καλεῖται: ὁμοίωμα τοῦ γραμμικοῦ ἐλατηρίου, ὁμοιόμορφοι τάσεις ἐφελκυσμοῦ καὶ κάμψεως ἐπιβάλλονται κατὰ τὸ πάχος τοῦ δοκιμίου τῆς ρηγματωμένης πλακός, τὰ μεγέθη τῶν ὁποίων ἐξαρτῶνται ἀπὸ τὴν μορφὴν τῆς ρωγμῆς καὶ τὰς ἰδιότητας τοῦ ὑλικοῦ. Αἱ τάσεις αὐταὶ συσχετίζονται κατὰ τοιοῦτον τρόπον, ὥστε αἱ θλιπτικαὶ τάσεις τῆς κάμψεως νὰ ἀντισταθμίζουν τὰς ἐφελκυστικὰς τάσεις εἰς τὸ ὑπόλοιπον μὴ ρηγματωμένον πάχος τῆς πλακός. Κατὰ τὸ ὁμοίωμα τοῦ Rice, ἐνῶ αἱ κατανομαὶ τῶν ἐφελκυστικῶν καὶ καμπτικῶν τάσεων ἱκανοποιοῦν κατὰ τὸ πλεῖστον τὰς συνθήκας εἰς τὸ μέτωπον τῆς ρωγμῆς κατὰ τὴν κεντρικήν της περιοχήν, ἀδυνατοῦν νὰ ἱκανοποιήσουν τὰς συνθήκας εἰς τὰ ἄκρα τῶν χειλέων τῆς ρωγμῆς. Πράγματι, εἰς τὰ ἀκραῖα αὐτὰ σημεῖα τὸ ὁμοίωμα αὐτὸ δέχεται μηδενικοὺς συντελεστὰς ἐντάσεως τάσεων, ἐνῶ εἰς τὴν πραγματικότητα εἰς τὰ σημεῖα αὐτὰ αἱ ἰδιομορφίαι τῶν τάσεων εἶναι σημαντικαί.

Κατὰ τὸ ὁμοίωμα, τὸ ὁποῖον εἰσάγομεν διὰ τῆς ἀνακοινώσεως αὐτῆς, δεχόμεθα κατανομὴν ἐφελκυστικῶν καὶ καμπτικῶν τάσεων, ὄχι εἰς τὰ ἀκραῖα σύνορα τῆς ρηγματωμένης πλακός, ἀλλὰ εἰς τὰ ἐμπρόσθια χείλη τῆς ρωγμῆς. Αἱ κατανομαὶ αὐταὶ εἶναι μεταβαλλόμεναι ἐκ τοῦ μέσου τῆς ρωγμῆς πρὸς τὰ ἄκρα της. Εἰς τὴν γειτονίαν τῶν ἄκρων τῶν χειλέων αἱ τάσεις αὐταὶ μεταβάλλονται ραγδαίως, τείνουσαι σχεδὸν ἀσυμπτωτικῶς πρὸς μεγάλας τιμάς. Κατ' αὐτὸν τὸν τρόπον ἐξασφαλίζεται ἡ εἰσαγωγὴ χαλαρῶν ἰδιομορφιῶν τῶν χειλέων τῆς ρωγμῆς καὶ ἰδιαιτέρως τῶν ἄκρων των.

Αἱ συναρτήσεις ποὺ ἐκφράζουν τὰς κατανομὰς αὐτὰς προσδιορίζονται διὰ τῶν ἀκραίων τιμῶν των καὶ τῆς μορφῆς των, ἡ ὁποία δίδεται ὡς δυώνυμον δυνάμεων. Μορφώνεται σύστημα ὁλοκληρωτικῶν ἐξισώσεων, ἐκφράζον τὸ ἀντίστοιχον πρόβλημα Hilbert τῇ βοηθείᾳ τῶν μιγαδικῶν δυναμικῶν τῶν τάσεων κατὰ Muskhelishvili.

Αἱ ὁλοκληρωτικαὶ ἐξισώσεις λύονται ἀριθμητικῶς καὶ προσεγγιστικῶς, καὶ ἐκ τῆς λύσεώς των ὁρίζονται ὄχι μόνον ἡ μεταβολὴ τοῦ συντελεστοῦ ἐντάσεως τῶν τάσεων κατὰ μῆκος τοῦ μετώπου τῆς ρωγμῆς, ἀλλὰ καὶ ἡ διανομὴ τῶν τάσεων καὶ παραμορφώσεων εἰς ὅλον τὸ πεδίον τῆς πλακός.

Τὰ ἀποτελέσματα ποὺ εὑρέθησαν εἰς σχετικὰ ἀριθμητικὰ παραδείγματα εἶναι ἱκανοποιητικὰ καὶ συμφωνοῦν μέ τινα ἤδη εὑρεθέντα, ἀλλὰ καὶ μὲ ἄλλα προκύπτοντα ἀπὸ διαφόρους πειραματικὰς μεθόδους, εἰς τρόπον ὥστε νὰ θεωρεῖται ὅτι ἡ μέθοδος αὐτὴ ἀποτελεῖ βασικὴν πρόοδον εἰς τὴν ἐπίλυσιν τοῦ δυσκόλου καὶ ἐνδιαφέροντος προβλήματος τῆς ἐντατικῆς καταστάσεως τῆς ἀναπτυσσομένης εἰς μερικῶς ἐπιφανειακὰς ρωγμὰς εἰς τὰς κατασκευάς.

REFERENCES

1. J. R. Rice and N. Levy, "The part-Through Surface Crack in an Elastic Plate", Jnl. Appl. Mech., Trans ASME, Vol. 39, No. 2, pp. 185 - 194, 1972.
2. G. R. Irwin, "Crack Extension Force for a Part-Through Crack in a Plate", Jnl. Appl. Mech., Trans. ASME, Vol. 33, No. 4, pp. 651 - 654, 1966.
3. A. E. Green and I. N. Sneddon, "The Distribution of Stress in the Neighbourhood of a Flat Elliptical Crack in an Elastic Solid", Proc. Cambridge Phil. Soc., Vol. 46, pp. 159 - 163, 1960.
4. F. W. Smith, "The Elastic Analysis of the Part-Circular Surface Flaw Problem by the Alternating Method", The Surface Crack : Physical Problems and Computational Solutions, J. L. Swedlow Editor, ASME Publ., New York, pp. 125 - 152, 1972.
5. F. W. Smith, and M. J. Alavi, Stress Intensity Factors for a Penny-Shaped Crack in a Half-Space, Engrg. Fract. Mech., Vol. 3, No. 3, pp. 241 - 254, 1971.
6. F. W. Smith and M. J. Alavi, "Stress Intensity Factors for a Part-Circular Surface Flaw", Proc. First Intern. Conf. Pressure Vessel Technology, ASME, N. York, pp. 793 - 800, 1969.
7. R. W. Thresher and F. W. Smith, "Stress Intensity Factors for a Surface Crack in a Finite Solid", Jnl. Appl. Mech., Trans. ASME, Vol. 39, No. 1, pp. 195 - 200, 1972.
8. R. C. Shah and A. S. Kobayashi, "Stress Intensity Factor for Elliptical Crack Under Arbitrary Normal Loading", Engrg. Fract. Mech., Vol. 3, No. 1ι pp. 71 - 96, 1971.
9. R. C. Shah and A. S. Kobayashi, "Stress Intensity Factors for an Elliptical Crack Approaching the Surface of a Semi-infinite Solid", Intern. Jnl. Fracture, Vol. 9, No. 2, pp. 133 - 146, 1973.
10. R. C. Shah and A. S. Kobayashi, "On the Surface Flaw Problem", The Surface Crack: Physical Problems and Computational Solutions, J. L. Swedlow Editor, ASME Publ., New York, pp. 79 - 124, 1972.
11. R. J. Hartranft and G. C. Sih, "Alternating Method Applied to Edge and Surface Crack Problems", Methods of Analysis and Solutions of Crack Problems, G. C. Sih Editor, Noordhoff Intern. Publ. The Netherlands, pp. 79 - 238, 1973.

12. C. M. Segedin, "A Note on Geometric Discontinuities in Elastostatics", Intern. Jnl. Engrg. Sci., Vol. 6, pp. 309 - 312, 1968.

13. H. Miyamoto and T. Miyoshi, "Analysis of Stress Intensity Factor for Surface-Flawed Tension Plate", High-Speed Computing of Elastic Structures, Proc. of IUTAM Symposium, Univ. of Liege, pp. 137 - 155, 1971.

14. J. Heliot - R. C. Labbens and A. Pellisier - Tanon, "Semi-Elliptic Cracks in a Cylinder Subjected to Stress Gradients", Fracture Mechanics, ASTM Spec. Techn. Publ. 677, pp. 341 - 364, 1979.

15. T. A. Cruse, "Numerical Solutions in Three-Dimensional Elastostatics", Intern. Jnl. Sol. Struct., Vol. 5, pp. 1259 - 1274, 1969.

16. T. A. Cruse, "Numerical Evaluation of Etastic Stress Intensity Factors by the Boundary Integral Equation Method", The Surface Crack: Physical Problems and Computational Solutions, J. L. Swedlow Editor, ASME Publ., New York, pp. 153 - 170, 1972.

17. H. Tada - P. C. Paris and G. R. Irwin, "The Stress Analysis of Cracke", Handbook, Del. Res. Corp., Hellertown, Pennsylvania, 1973.

18. F. Delale and F. Erdogan, "Application of the Line-Spring Model to a Cylindrical Shell Containing a Circumferential or Axial Part-Through Crack", Jnl. Appl. Mech., Trans. ASME, Vol. 49, No. 1, pp. 97 - 102, 1982.

19. D. M. Parks, "Inelastic Analysis of Surface Flaws Using the Line-Spring Model", Proc. Fifth Intern. Conf. on Fracture, Cannes, France, D. François, Editor, Pergamon Press London Publ., Vol. 5, pp. 2589 - 2598, 1981.

20. J. P. Benthem, "State of Stress at the Vertex of a Quarter - Infinite Crack in a Half - Space", Int. J. Solids and Structures, Vol 13, pp. 470 - 492, 1977; see also : Bazant, Z. P. and Estenssoro, L. F., "General Numerical Method for Three Three - Dimensional Singularities in Cracked or Notched Elastic Solids", Fracture, Vol. 3, ICF 4, Waterloo, Canada, June 19 - 24, pp. 371 - 385, 1979.

21. P. H. Francis and D. L. Davidson, "Experimental Chracterization of Yield Induced by Surface Flaws", The Surface Crack, Physical Problemφ and Computational Solutions, J. R. Swedlow Editor, ASME Publ. N. York, pp. 63 - 67, 1972.

22. P. C. Paris and G. G. Sih, "Stress Analysis of Crack, Fracture Toughness Testing and Its Applications", ASTM STP. 381 pp. 30 - 83, 1964.

23. C. W. Smith - W. H. Peters and G. C. Kirby, "Crack-Tip Measurements in Photoelastic Models", Experimental Mechanics, Vol. 22, N8. 12, pp. 448 - 451, 1982.

24. P. S. Theocaris, "The Method of Reflected Caustics for the Study of Part-Through Circular Cracks", Proc. Nat. Acad. Athens, Vol. 90, No. I, pp. 210 - 215, 1983.

25. N. I. Muskhelishvili, "Some Basic Problems of the Mathematical Theory of Elasticity", Noordhoff, Groningen, 1953.

26. G. Berger - H. P. Keller and D. Munz, Determination of Fracture Toughness with Linear Elastic and Elastic-Plastic Methods", Elastic-Plastic Fracture, ASTM STP 668, J. D. Landes, J. A. Begley and G. A. Clarke Efs. Amer. Soc. Test. Mat. Publ. pp. 378 - 405, 1979.

27. J. F. Knott, "Macroscopic Aspects of Crack Extensions", Advances in Elasto-Plastic Fracture Mechanics, L. H. Larsson Ed., Applied Science Publ. London, pp. 1 - 20, 1980.

28. T. Nishioka and S. N. Atluri, "Analytical Solution for Embedded Elliptical Cracks and Finite-Element Alternating Method for Elliptical Surface Cracks Subject to Arbitrary Loadings", Engrg. Fract. Mech., Vol. 17, No. 3, pp. 247 - 268, 1983.

29. S. Bhandari and J. Jalouneix, "On the Front-Surface Correction Factor for Semi-elliptical Surface Cracks", Intern, Jnl. Fract. Vol. 18, No. 1, pp. R 9 - R 16, 1982.

30. F. Delale and F. Erdogan, "Line Spting Model for Surface Cracks in a έeissner Plate", Intern. Jnl. Engrg. Sci., Vol. 19, pp, 1331 - 1340, 1981.

31. J. C. Newman Jr. and I. S. Raju, "Analysis of Surface Cracks in Finite Plate Under Tension or Bending Loads", NASA Technical Note No. 1758, 1979.

32. R. I. Hartranft and G. C. Sih, "An Approximate Three-Dimensional Theory of Plates with Application to Crack Problems", Intern. Jnl. Engrg. Sci., Vol. 8, pp. 711 - 729, 1970.

33. G. C. Sih, "A Review of the Three-Dimensional Stress Problem for a Cracked Plafe", Intern. Jnl. Fract. Mech., Vol... 7, pp. 39 - 61, 1971.

34. J. C. Bell, "Stress Analyses for Structures with Surface Cracks", NASA CR-15 400, NASA Lewis Res. Center (Aug. 1978).